



Stockholm
University

Bachelor Thesis

Degree Project in
Geoscience 15 hp

Reconstruction of past atmospheric mineral dust over the last 5200 cal yr BP using geochemical proxies from Store Mosse, Sweden

Oskar Vikdahl



Stockholm 2021

Department of Geological Sciences
Stockholm University
SE-106 91 Stockholm

Abstract

Ombrotrophic peat bogs only receive minerogenic input from atmospheric deposition, have a wide spatial distribution and provide continuous and high-resolution records of atmospheric dust. To date, only a small portion of the extensive Store Mosse mire complex has been studied with the intentions of identifying periods of increased dust deposition. Here, changes in atmospheric paleodust in the northern part of Store Mosse (57° 17' 7.69''N, 13° 54' 8.79''E), covering the last 5200 calendar years before present (cal yr BP) was reconstructed from a peat core. Multiple proxies were used to determine peatland development and mineral dust deposition. Results from the bulk density, peat accumulation rate (PAR) and ash content suggests that the peatland started a transition from fen to bog at 3900 cal yr BP and was fully ombrotrophic at 3400 cal yr BP. Elemental data was acquired by using X-ray fluorescence core scanner (XRF-CS) on ashed peat samples. Bulk density, ash content and a suite of 11 elements were statistically evaluated using principal component analysis (PCA) to identify periods of dust deposition. From the peat paleodust reconstruction four dust events were recorded, 2300-1680, 1540-1440, 1300-1170 and 900-700 cal yr BP. The first period (2300-1680) is the longest in duration and presence of clay and heavy minerals (ilmenite) are inferred along with increased PAR. The other dust events are associated to coarser grains of quartz and feldspar. A total of ten periods with increase of coarse-grained quartz and feldspar during the last 2700 cal yr BP are connected to short lived periods of increased storminess. Good agreement in these periods are seen in a nearby record (Gåling, 2019), and from two ombrotrophic bogs ca 90 km southwest of Store Mosse (Björck and Clemmensen 2004), thus suggesting that the storms were of regional scale.

Keywords

Atmospheric dust, ombrotrophic peat, XRF, geochemistry, storminess, paleoenvironment, Store Mosse

Contents

1. Introduction	4
1.1 Site description	6
2. Methods	7
2.1 Sampling.....	7
2.2 Bulk Density, true depth and ash content	8
2.3 Age model	8
2.4 X-ray fluorescence core scanner (XRF-CS)	9
2.5 Statistical analysis Principal Component Analysis (PCA).....	9
3. Result	9
3.1 Age-depth modeling	9
3.2 Bulk Density and Peat Accumulation Rate (PAR).....	10
3.3 Ash content and Elemental Data XRF-CS	11
3.4 Statistical analysis on XRF-CS data	12
3.5 Elemental Ratios	14
3.6 Biplots of elemental data.....	16
4. Discussion.....	16
4.1 Peatland Development	16
4.2 Interpretations of the geochemical signals in the SM-DN peat core.....	17
4.3 Dust Events	19
4.4 Comparison with other paleoenviromental records	21
5. Conclusions	22
Acknowledgement	23
5. References	23
6. Appendix	26
Appendix A, Fresh core photos.....	26
Appendix B, Elemental profiles.....	27

1. Introduction

Atmospheric mineral dust plays a crucial role within the climate system, acting as both a forcing and feedback mechanism (Albani et al., 2015). Dust particles in the atmosphere affect energy distribution within the climate system by absorbing and scattering incoming solar radiation, providing cloud formation nuclei, through chemical reactions in the atmosphere and by acting as a source of nutrients to the biosphere (Kohfeld and Harrison, 2001; Shao et al., 2011). Given these complex direct and indirect roles in the climate system, there is a need to understand spatial and temporal variations in dust deposition globally.

Most studies examining past changes in atmospheric dust have been carried out on marine sediments and ice core records from the poles despite approximately 75 % of all atmospheric dust is deposited onto land (Kohfeld and Harrison, 2001; Shao et al., 2011). Atmospheric dust can be hard to detect in lake and marine sediment due to sedimentary input from other sources and mixing. Ice cores provide long undisturbed sequences of dust deposition but are spatially restricted to the poles (Lambert et al., 2008). The main terrestrial paleodust record to date has been loess. Loess are unevenly distributed over the continents as well as being hard to interpret because they can act as both source and sinks and are subject to mixing of dust from different sources (Albani et al., 2015; Kohfeld and Harrison, 2001). Since the beginning of the 21st century however, paleodust records from peat bogs have been increasingly compiled by using different proxies connected to the atmospheric dust (e.g., geochemistry, grain size, mineralogy).

Peatlands develop mainly in cold-temperate boreal climates where we often find previously glaciated landscapes (Kylander et al., 2018). Mid- and northern latitudes are often wet and cold which provide optimal conditions for peat accumulation. Peatlands have long been considered valuable records of past climate (Björck and Clemmensen, 2004). Blytt (1876) recognized in the late 19th century how the stratigraphy of peat was linked to drier and wetter conditions during the Holocene. Since then, multiple studies have been carried out on ombrotrophic bogs to identify how the atmospheric dust and peat properties are connected to past climate (e.g., de Jong et al., 2006; Kylander et al., 2013; Sjöström et al., 2020).

Ombrotrophic peat bogs only receive minerogenic input from atmospheric deposition. This makes peat bogs to excellent archives of past dust deposition. Bogs commonly develop from fens which are more nutrient rich compared to the nutrient poor bogs (Svensson, 1988). This is because the fen can receive input from additional sources such as ground or surface water. For a fen to develop into a bog with an ombrotrophic status can be a result of either a lowered water table or peat accumulation that disconnects the fen from the water supply below (Franzén, 2006). Ombrotrophic peat bogs have a wide spatial distribution and provide continuous and high-resolution records of atmospheric dust. Since the dust is entrapped in the organic matter-rich matrix (at times up to 99%) and buried as the peatland develops, radiocarbon (¹⁴C) dating can be performed with high accuracy.

The reconstruction of variations in dust deposition in peat based studies has often relied on geochemical proxies. All elements deposited onto the bog surface are not however, expected to be preserved within the peat since the high acidity of the bog may dissolve minerals that are sensitive to low pH, such as carbonates for example (Franzén, 2006). Some elements like N, P and K are essential nutrients to plants, and will therefore be recycled within the peat record. Lastly, due to the fluctuating water tables near the surface, some redox sensitive elements are mobile in the peat record (e.g., Fe and Mn). To track dust signals within the peat record,

researchers rely on elements that are biogeochemically conservative and non-mobile in the peatland (Kylander et al., 2016; Sjöström et al., 2020).

The amount and composition of atmospheric dust greatly varies with time, climate, and location on earth (Kohfeld and Harrison, 2001). Lower latitudes are generally dustier compared to higher latitudes because of the drier climate and larger extent of dust source areas (deserts). During dry periods, vegetation cover and soil moisture is reduced, making the particles soils and sediments more available for aeolian transport. Wetter climates have the opposite effect and is connected to increased vegetation cover and therefore less loose sediment available for transport (Albani et al., 2015). Deposition of the dust can either be by wet or dry deposition. Apart from climate factors, human activities such as industrialization, agriculture, drainage and deforestation also affect the available atmospheric dust. Industries emit pollution particles into the air, agriculture and draining make the soil more susceptible to erosion and deforestation opens the landscape making it more accessible to wind (Björck and Clemmensen, 2004; Vandel et al., 2019).

Aeolian transport of a range of different sized particles is possible, where stronger winds have the potential to carry larger grain size fractions. Dust which has been transported more than 100 km mostly contains grains less than 4 μm and few grains larger than 16 μm . On shorter distances larger grain sizes up to >200 μm are possible but generally fractions <100 μm are seen. However, this is highly dependent on location and available source (Pye, 1987). Stronger winds are often associated with storm systems. Within the climate systems storms are responsible for redistributing the energy and momentum that is created by differential heating of the equator and the poles (Shaw et al., 2016). Thus, processes that affect the thermal gradient have potential to influence storminess (a term explaining intensity and frequency of storms) and storm track position.

Reconstruction of past storminess using peat paleoarchives is a relatively new tool and adds another layer of interpretation to paleodust studies. The first peat based storm reconstruction was published by Björk and Clemmensen in 2004 using a core from a coastal bog in Halland. Studies from (Jong et al., 2006) and (Björck and Clemmensen, 2004) both used a grain size approach to identify periods of storminess with the basic premises that stronger winds can carry larger particles. In 2013 (Kylander et al., 2013) compiled the first dust record in Sweden from an ombrotrophic bog using conservative elemental geochemistry on a peat core retrieved from Store Mosse in Småland, south central Sweden. The result from this study combined with a later study by (Kylander et al., 2016) performed on the same peat sequence, the SM-S core, identified four periods of increased atmospheric deposition since 8500 calendar years Before Present (cal yr BP). One of these dust events (DE) was linked to stormier conditions in the mid-Holocene (DE2 from 5300 to 4370 cal yr BP). To date, only a small portion of the extensive Store Mosse mire complex, covering 77 km², has been studied with the intentions of identifying periods of increased dust deposition.

While research at Store Mosse has been on-going for decades, much of the focus has been on the southern end of the peat bog where the thickest and oldest deposits have been found (Kylander et al., 2018, 2016, 2013). Further north a small creek (Blådöpet) (Fig.1) runs from lake Kalvasjön in a southwestern direction where fen conditions prevail. In the northernmost part of Store Mosse aeolian derived sand is commonly interrupting the otherwise dominating peat (Fig.1).

In 2017 a core (Store Mosse Dune South or SM-DS) was taken just south of the bisecting dune system in the northern section of the mire complex (Fig 1). Using the mineral fraction after dry ashing, Gåling (2019) analysed samples with Attenuated Total Reflection-Fourier Transform Infrared Spectroscopy (ATR-FTIR) and X-ray Fluorescence Core Scanning (XRF-CS). Principal Component Analysis (PCA) was used to interpret the elemental data (XRF-CS) and spectral data (ATR-FTIR) separately. The results from the XRF-CS and ATR-FITR identified changes in mineralogy which were then linked to different wind intensities. The results from the SM-DS core correlated well with the record from the coastal bog in Halland done by Björck and Clemmensen (2004).

A potential source of the different minerals observed in the SM-DS record is the dune system bisecting the northern part of Store Mosse. A record from the north side of the dunes could be expected to show similar signals as on the southern side of the dunes. The area north of the dune system has been left unstudied since research started almost a century ago. To date we know little about the peatland development and past changes in dust deposition captured in the northern part of Store Mosse. With this in mind, the objectives of this study are to:

- 1) Build an understanding of peatland development in the northernmost basin at Store Mosse using a combination of bulk density, ash content and peat accumulation rates (PAR)
- 2) Understand the processes controlling the geochemical signals archived in the peat
- 3) Examine atmospheric dust and what controls this
- 4) Compare with other paleoenvironmental records from locations nearby

This project will be based on a peat core (Store Mosse-Dune North or SM-DN) just north of the bisecting dune system in Store Mosse. Before the start of this project, the SM-DN core was subsampled (2 cm resolution), freeze-dried and ^{14}C dated. Fieldwork and coring had already been carried out in 2017.

1.1 Site description

Store Mosse (57° 17' 7.69''N, 13° 54' 8.79''E) is an ombrotrophic peatland located in Småland, southern Sweden (Fig 1). The peatland is situated around 160-170 m above sea level (Svensson, 1988) with an annual average temperature of 5.9°C and precipitation of 716 mm where most of the precipitation occurs during the summer (SMHI, 2021). Store Mosse experiences a temperate climate with cool summers and mild winters. The surrounding bedrock consists mostly of granite but also granodiorite, syenitoid, quartz monzodiorite and metamorphic equivalents that formed 1.7 Ga during the Sveconorwegian orogeny. The lithology is locally interrupted by more mafic bedrocks such as gabbro, pyroxenit, anorthosite, dolerite and granophyric granite which has been dated to 1.6 Ga (Geological Survey of Sweden, 2020a).

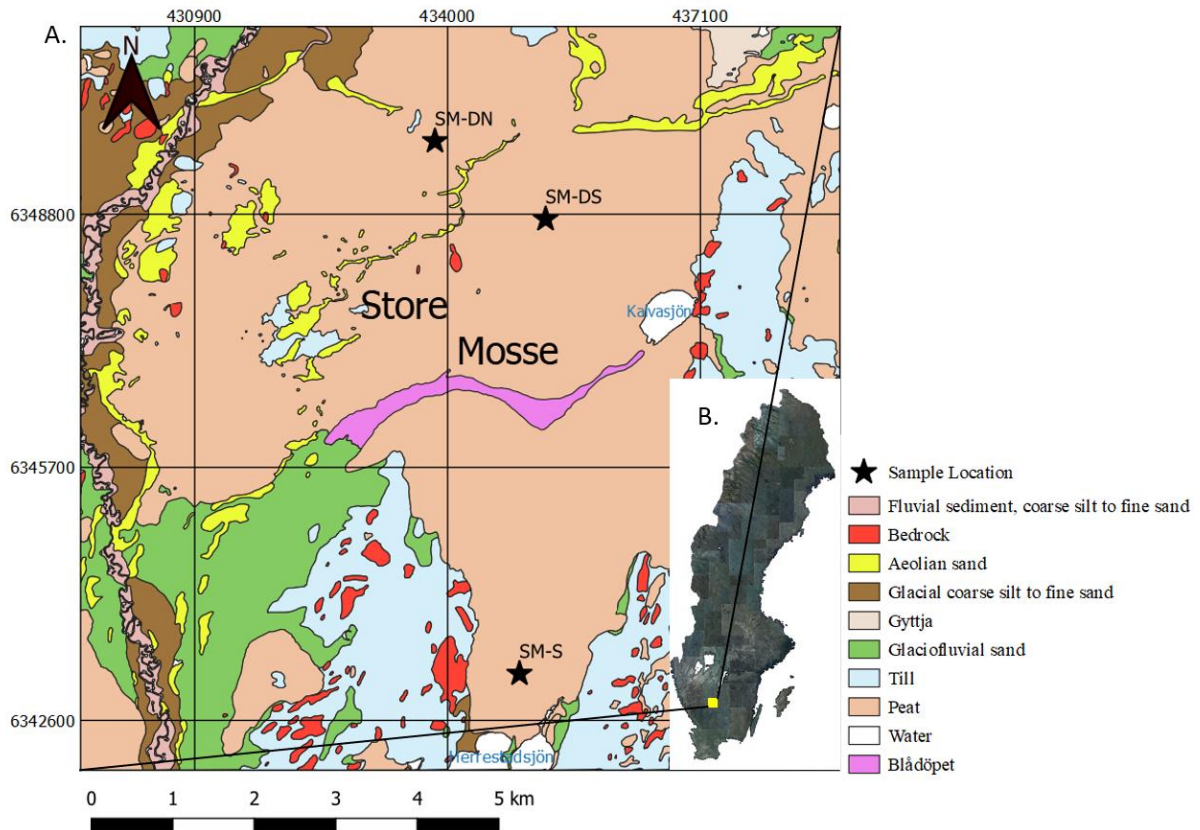


Figure 1. A) Soil map and location of the sample core SM-DN, SM-DS (Gåling, 2019) and SM-S (Kylander et al. 2013). B) Orientation map. Soil map was created using QGIS version 13.10, Jordartskartan 1:25 000-1:100 000 vektor data from ©Sveriges geologiska undersökning. Orientation map orthophoto from ©Lantmäteriet. Projected coordinate system: SWEREF99TM.

After deglaciation ca 14 ka (Ising, 2001; Lundqvist and Wohlfarth, 2000), Store Mosse was covered by an ice lake known as Fornbolmen. Due to the bedrock topography and isostatic rebound the lake was drained southwards leaving a bare lake bottom. The formation of sand dunes that bisects Store Mosse today are still unclear. The dunes are believed to have formed by aeolian reworking of the bare lake bottom or from glaciofluvial material in the northern edge of the bog. Peat formation began on the southern open sandy areas (Svensson, 1988), however, it is only after dune emplacement peat proximal to the dunes starts to accumulate, ca 5000 cal yr BP (Gåling, 2019). Postglacial till and glaciofluvial sediment are the predominant sediments surrounding the Store Mosse (Geological Survey of Sweden, 2020b).

2. Methods

2.1 Sampling

Sampling was carried out in September 2017 in the northern part of Store Mosse just north of the bisecting dune field. The SM-DN core was recovered using a Russian corer with a diameter of 7.5 cm. Six 1 m sections with 25 cm overlap were taken from two alternating holes to a depth of 508 cm. The SM-DN core was sub-sampled using a stainless-steel knife into a contiguous record with 2 cm resolution. From each of the slices a cube of approximately 1 cm³

was cut out. The cubed sample were put into pre-weighed zip-lock bags while the rest of the slice was put into a separate zip-lock bag to be used for calculating the bulk density and for the geochemical analyses, respectively. All samples were then frozen for 24-hours prior to freeze-drying. All samples were put into the freeze-drier for at least four days to remove all the water content.

2.2 Bulk Density, true depth and ash content

After all the samples had been freeze-dried the cubed samples were weighed and measured. The weight of the plastic bag was subtracted from the total weight to obtain the dry weight of the cubed samples. Each cube was measured (width * height * length) with a calliper to estimate its volume. The bulk density (g/cm^3) was calculated by dividing the dry weight of a cubed sample with its estimated volume ($\pm 10\%$).

Due to irregularities when coring, the true depth of the SM-DN core was established using the bulk density measurements of the subsamples. Overlapping measurements were used for alignment of the core as well as visual assessment of freshly taken photos of the core (Appendix A, Fig A1). The total composite depth or true depth after alignment was 490 cm. Note that the top 50 cm was not collected.

Dry ashing of the samples was done every at 5 cm of the composite core. Crucibles were pre-dried in an oven for 105°C for at least 4 hours to remove any water before being put in a desiccator to cool. All crucibles were then weighed. All samples ($n = 128$) were put in the crucibles and dried in an oven for 105°C for at least 4 hours before being put in a desiccator to cool and then weighed. The crucible's weight was subtracted to get the dry weight of each sample. All the samples were put in a 500°C oven overnight to fully incinerate the samples. The samples were once again put in a desiccator to cool and then weighed. The ash content was calculated as a percentage of the dry weight of a sample which indicates how much inorganic material each sample contains.

2.3 Age model

The age model was created by using two ^{14}C dates measured on plant macrofossil remains. A software called R Bacon was used by J. Sjöström to create the age model. All ages are presented in cal yr BP.

2.4 X-ray fluorescence core scanner (XRF-CS)

The XRF-CS analysis was carried out on the ashed samples (5 cm resolution) using an Itrax core scanner at the Geological Department of Science, Stockholm University, Sweden. The ash was loaded into plastic sample boats that have an inner dimension of 8 mm x 2 mm x 2 mm depth (Fig 2). Labware was cleaned with ethanol between each sample. The XRF-CS analysis on the ashed samples were done at a voltage of 30 kW and a current 40 mA with a step-size of 500 μ m for 50 seconds. The core scanner analyses across the entire tray of samples and the spectra belonging to the plastic is removed. Only one spectra per sample is used. Traditionally XRF-CS are performed directly on the core surface. However, because peat cores often exhibits uneven surfaces and are high in water and organic content, the ability to reproduce elemental compositions are not optimal (Longman et al., 2019).



Figure 2. Ashed samples in sample boats.

2.5 Statistical analysis Principal Component Analysis (PCA)

PCA is a statistical method that can be used to explain variance among samples as well as identify major trends in data. The PCA was based on the bulk density, ash content and the elemental data generated from the XRF-CS. Using the JMP 16 software the PCA was performed with a varimax orthogonal rotation. The number of factors was based on Eigenvalues (> 1) and interpretation of the raw data. Peak area (pa) values from XRF-CS analysis, bulk density and ash content were converted into z-scores to avoid scaling by transforming values to average-centred distributions. To calculate the z-scores the following formula was used:

$$Z=(X-\mu)/\sigma$$

Z represents the z-score, X is the value at each data point, μ is the average of each variable and σ is the standard deviation of each variable.

3. Result

3.1 Age-depth modeling

Two radiocarbon dates were acquired for the SM-DN sequence. The lowermost sample at 490 cm depth was dated to 5169 cal yr BP. The second radiocarbon date was taken from the middle of the core at 324 cm depth and was dated to 2828 cal yr BP. The result from the age depth model is shown in (Fig 3).

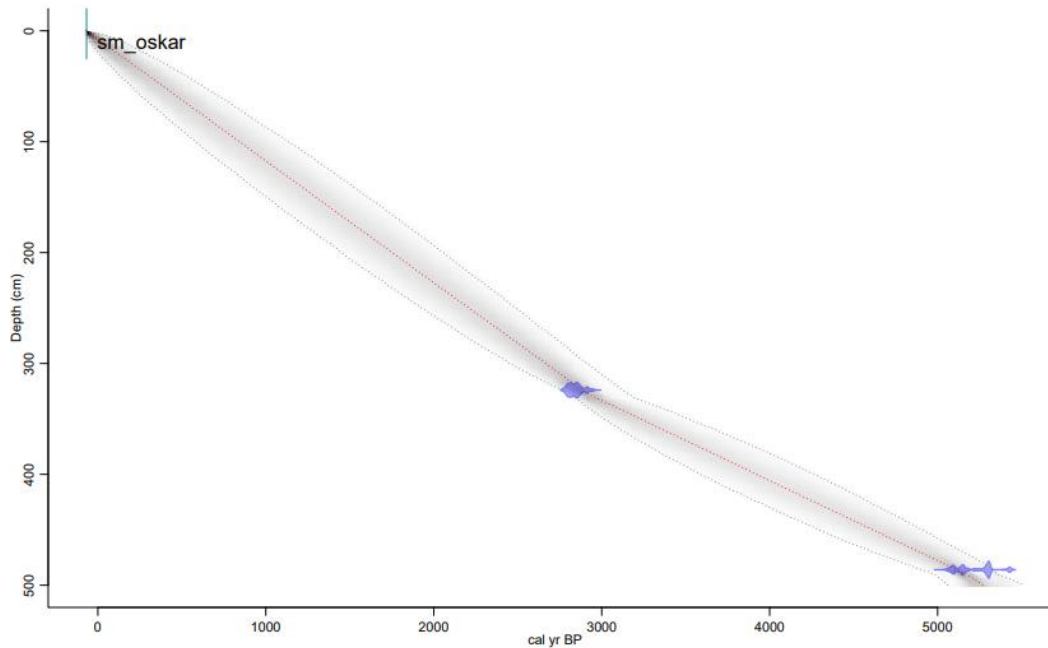


Figure 3. Age-depth model based on two ^{14}C dates. Modeling performed by Jenny Sjöström in the RBacon software. Blue is the ^{14}C dates, the mean age is shown with red dotted line, while the outer dotted line is the 95% confidence interval.

3.2 Bulk Density and Peat Accumulation Rate (PAR)

Bulk densities range from $0.04\text{-}0.30\text{ g/cm}^3$ with an average value of $0.12\pm 0.06\text{ g/cm}^3$ ($n = 219$) (Fig 4). The bulk density values are the highest at the base of the profile ($0.16\text{-}0.30\text{ g/cm}^3$) to 3840 cal yr BP where the maximum value is observed at 5140 cal yr BP . From 3840 cal yr BP a two-step rapid decrease in bulk density occurs over a period of 440 years that stabilizes around 0.88 g/cm^3 at 3400 cal yr BP . The following 900 years, until 2500 BP only small variations ($0.06\text{-}0.09\text{ g/cm}^3$) in the bulk densities are seen. A gradual increase with one sharp shift at 2350 cal yr BP marks the period $2500\text{-}2200\text{ cal yr BP}$. The period $2200\text{-}1900\text{ BP}$ show elevated values in bulk density and begins with a sharp increase from 0.10 to 0.17 g/cm^3 from where values start to fluctuate between $0.16\text{-}0.22\text{ g/cm}^3$ until the period ends with a sharp decrease down to 0.10 g/cm^3 . This is followed by a similar looking sequence for $1900\text{ - }1600\text{ cal yr BP}$ that begins with a sharp increase (up to 0.18 g/cm^3), ends with a sharp decrease (down to 0.08 g/cm^3). The following 200 years show a gradual increase from followed by a sharp decrease down to 0.05 g/cm^3 . The period from $1400\text{ - }400\text{ cal yr BP}$ represents the minimum values in the profile, ranging from $0.09\text{-}0.04\text{ g/cm}^3$. The lowest bulk density is found at 650 cal yr BP . During this period, the profile shows four significant peaks with increasing bulk density, occurring at $1250, 950, 660$ and 500 cal yr BP .

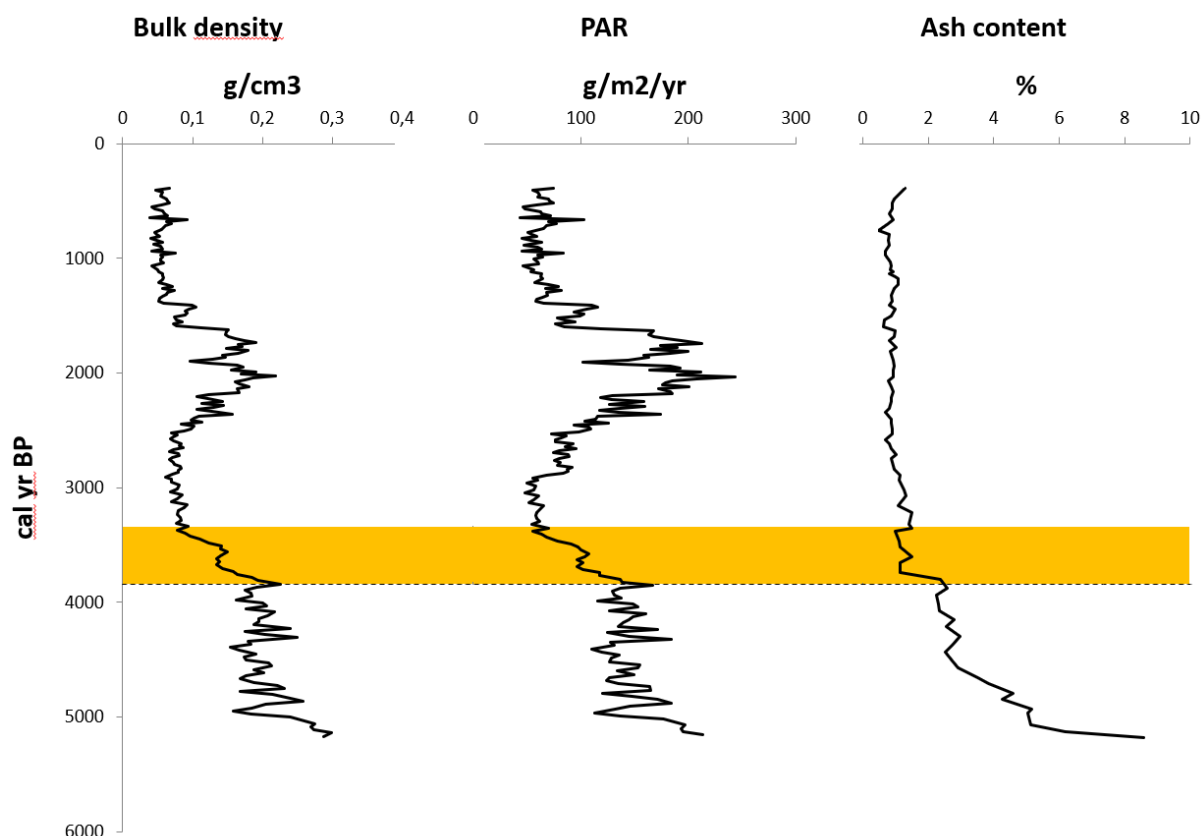


Figure 4. Organic peat proxies (bulk density and PAR) and inorganic peat proxy ash content. Black dashed line represents the start of the fen-bog transition and orange area the time for the transition to finish into a fully ombrotrophic bog.

The PAR is calculated by multiplying the bulk densities with the thickness (2 cm) of the sample and dividing by the age difference between each sample. Because the age-depth model is almost linear, the PAR profile follows the trend of the bulk density profile. The average peat growth at SM-DN is 0.95 cm/yr with PAR values ranging from 43-243 g/m²/yr with an average of 108±47 g/m²/yr (n = 218). At the base of the profile high values of PAR with high variability are observed between 5150-3850 cal yr BP. 3840-3400 cal yr BP marks a period of rapid decrease in PAR. A stable period of lower values persists 3400-2500 cal yr BP followed by a clear gradual increase for 300 years. The following 800 years, two periods of increased PAR (2200-1900 and 1900-1600 cal yr BP) are observed where the maximum value for the sequence is observed at 2000 cal yr BP. Low values with low variability take place from 1400-400 cal yr BP. Peaks are seen at 1250, 950, 660, 500 cal yr BP in the uppermost section of the profile.

3.3 Ash content and Elemental Data XRF-CS

Ash content in the SM-DN profile (Fig 4) ranges from 0.5-8.6% with an average value of 1.6±1.6% (n = 91). High values are seen at the base of the profile where there is a gradual decline in ash content from 5100-3900 cal yr BP. At 3900 cal yr BP a sharp decrease in ash content marks the split between generally high and low values from which the ash content is relatively stable around 1±0.5% for the rest of the sequence. Four periods of short increase in ash content are observed at 3400-3150, 2600-2350, 1150-1250 cal yr BP, up to 1.5% where

values more commonly are < 1%. A trend of increasing ash content can be seen at the top of the profile from 500 cal yr BP towards present time.

The XRF-CS data is given as peak areas (pa). The data is semi-quantitative and shows relative changes in elemental concentration for the ashed samples throughout the profile. Elemental profiles for Al, Si, K, Ca, Ti, Mn, Fe, Ni, Cu, Zn, Rb, Sr and Pb were plotted against depth/age (Appendix B, Fig B1).

3.4 Statistical analysis on XRF-CS data

Based on the analytical performance of the elemental data (signal above background noise) and relevance to the scientific question Al, Si, K, Ti, Mn, Fe, Cu, Zn, Rb, Sr, and Pb were selected from the XRF-CS dataset together with peat properties (bulk density and ash content) for PCA. Two separate PCA were performed on the SM-DN data. The first PCA covers the entire sequence, denoted PC₅₁₀₀ (Fig 5) where three factors (PC₁₅₁₀₀-PC₃₅₁₀₀) explain 81.9% of the variance (Table 1). The second PCA covers that last 3400 cal yr BP, denoted PC₃₄₀₀ (containing ombrotrophic peat only Fig 5). Here four factors (PC₁₃₄₀₀-PC₄₃₄₀₀) were extracted that explained 84.3% of the variance (Table 2).

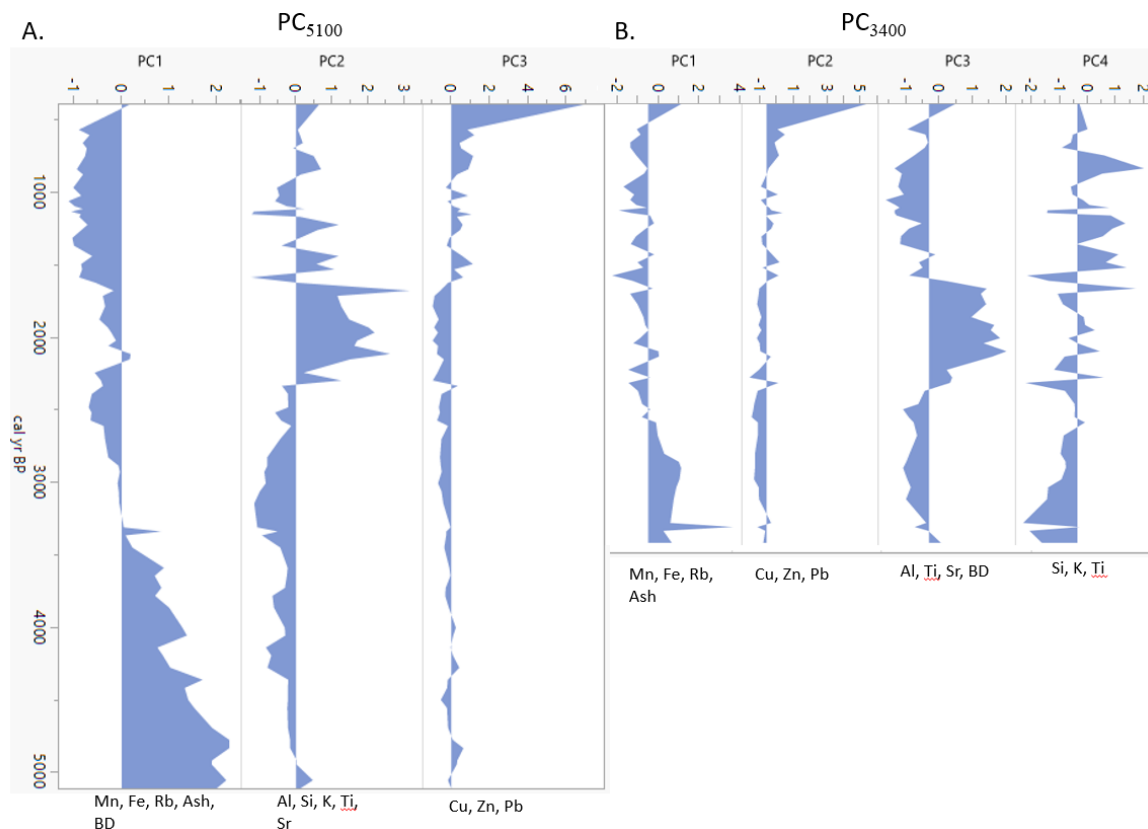


Figure 5. A) Factor scores for PC₅₁₀₀. B) Factor scores for PC₃₄₀₀. Associated variables (> 0.5) indicated below each PC. Bulk density (BD). All scores are plotted against age.

Table 1.

Result of PC₅₁₀₀ analysis. Strong association (> 0.5) within factors are indicated by bold.

Factor	PC1	PC2	PC3
Percentage	38.5	26.1	17.4
Cumulative %	38.5	64.6	81.9
Variable			
Al	0,38	0,86	0,01
Si	-0,56	0,6	0,36
K	-0,62	0,65	0,07
Ti	0,018	0,93	0,16
Mn	0,93	-0,08	0,17
Fe	0,91	-0,23	-0,13
Cu	-0,1	0,45	0,75
Zn	-0,14	0,14	0,9
Rb	0,91	-0,05	0,04
Sr	-0,35	0,78	0,22
Pb	0,18	-0,01	0,77
Ash	0,89	-0,06	0,05
Bulk Density	0,81	0,32	-0,21

PC1₅₁₀₀ represents 38.5% of the variance and is strongly positively associated (> 0.5) with Mn, Fe, Rb, ash content and bulk density while Si and K are strongly negatively associated (< -0,5). From 5100-3400 cal yr BP PC1₅₁₀₀ has positive factor scores that gradually decrease from 5100-3400 cal yr BP. From 3400-400 cal yr BP the factor scores are negative with one exception at 2100 cal yr BP where a peak with positive factor score occurs.

PC2₅₁₀₀ captured 26.1% of the variance and strongly associated elements include Al, Si, K, Ti and Sr. At the base of the profile a small positive peak is seen at 5000 cal yr BP. The following period 4900-2300 cal yr BP only negative factor scores are observed. From this point on, the factor scores display high variability with four periods of positive factor scores (2300-1600, 1550-1400, 1300-1150 and 900-700 cal yr BP). Sharp peaks within the periods positive are seen at 2300, 2100, 1950, 1700, 1550, 1450, 1200 and 850 cal yr BP.

PC3₅₁₀₀ represents 17.4% of the variance and strongly associates with Cu, Zn and Pb. The factor scores are negative in the bottom of the profile until 2300 cal yr BP where a small positive peak interrupts the predominantly negative factor score. Following this, the factor scores are negative until 1600 cal yr BP when a shift to low positive scores is seen until a rapid increase just at the top of the profile.

Table 2.

Result of PC₃₄₀₀ analysis. Strong association (> 0.5) within factors are indicated by bold.

Factor	PC1	PC2	PC3	PC4
Percentage	23.6	21.4	20.7	18.6
Cumulative %	23.6	45.0	65.7	84.3
Variable				
Al	0,16	0,02	0,85	0,4
Si	-0,32	0,38	0,11	0,75
K	-0,14	-0,04	0,27	0,86
Ti	-0,16	0,2	0,71	0,57
Mn	0,79	0,36	0,13	-0,18
Fe	0,85	-0,32	-0,1	-0,31
Cu	-0,19	0,78	0,12	0,47
Zn	0,11	0,91	0,03	0,12
Rb	0,92	-0,07	0,00031	0,1
Sr	-0,02	0,29	0,69	0,44
Pb	0,08	0,88	-0,07	-0,05
Ash	0,8	0,11	-0,02	-0,18
Bulk Density	-0,02	-0,24	0,93	-0,17

PC1₃₄₀₀ is strongly associated with Mn, Fe, Rb and ash content. At the base of the profile the values are positive and generally decrease until 2600 cal yr BP where scores are predominantly negative for the rest of the profile with exceptions of low positive peaks at 2200, 1700, 1400, 1200 and 400 cal yr BP.

PC2₃₄₀₀ represents 21.4% of the variance and strongly associates with Cu, Zn and Pb. From 3400 cal yr BP scores are generally negative until 2300 cal yr BP where a small positive peak interrupts the predominantly negative factor scores. From this point upwards greater variability is seen with elevated values observed at 1600, 1200 and 800 cal yr BP. The period 800 cal yr BP towards present show a rapid increase in the factor score.

PC3₃₄₀₀ explains 20.7% of the variance and is associated with Al, Ti, Sr and bulk density. Negative scores are seen throughout the whole sequence with the exception for the period between 2300-1680 cal yr BP where positive values are seen.

PC4₃₄₀₀ represents 18.6% of the variance and is strongly associated with Si, K and Ti. This profile shows large variability in the data. Negative scores are seen from 3400 cal yr BP until 2650 cal yr BP from which ten short periods of elevated scores are seen between 2650-2590, 2380-2270, 2150-2060, 2020-1850, 1700-1640, 1560-1370, 1370-1160, 1120-1040, 950-720 and 590-420 cal yr BP.

3.5 Elemental Ratios

Three elemental ratios, Si/Ti, Si/Al and K/Al for the SM-DN peat profile were plotted (Fig 6). The Si/Ti ratio ranges from 0-0.38 with an average of 0.13. The lowest recorded values are found at the base of the profile between 5100 and 4300 cal yr BP. This is followed by two peaks that first gradually increase and then decrease between 4300 and 3300 cal yr BP. The

Si/Ti ratio thereafter shows a gradual increase until 1700 BP which was followed by a rapid increase. The highest values are observed between 1500-1000 cal yr BP after which the value generally decreases but with a peak observed at 570 cal yr BP.

The Si/Al ratio ranges from 0-13.9 with an average of 4.2. The lowermost part of the profile follows a similar pattern as the Si/Ti ratio with low values from 5100-3150 from where a slow gradual increase occurs until 1700 cal yr BP. From 1700-400 cal yr BP large variability within the profile is observed, with ratios shifting dramatically and overall higher values persisting. Peaks between 1700-1100 cal yr BP occur with approximately 100-year intervals at 1600, 1500, 1250 and 1100 cal yr BP. Lower values with great variability from 1100-400 cal yr BP is observed but a slowly increasing trend can be identified during this period.

The K/Al ratio ranges from 5.4-129.4 with an average of 49.2. Between 5100-3800 cal yr BP the values are low and stable, ranging from 5.4-13.0. This is followed by a period of 500 years where two peaks are observed at 3650 and 3450 cal yr BP. An almost linear trend of increasing values from 3300-2300 cal yr BP ends with a sharp decrease in value that stables around the average until 1600 cal yr BP where a sharp increase is observed. The period from 1500 to 400 cal yr BP shows a decreasing trend in values with peak values occurring at 1500, 1200 and 850 cal yr BP.

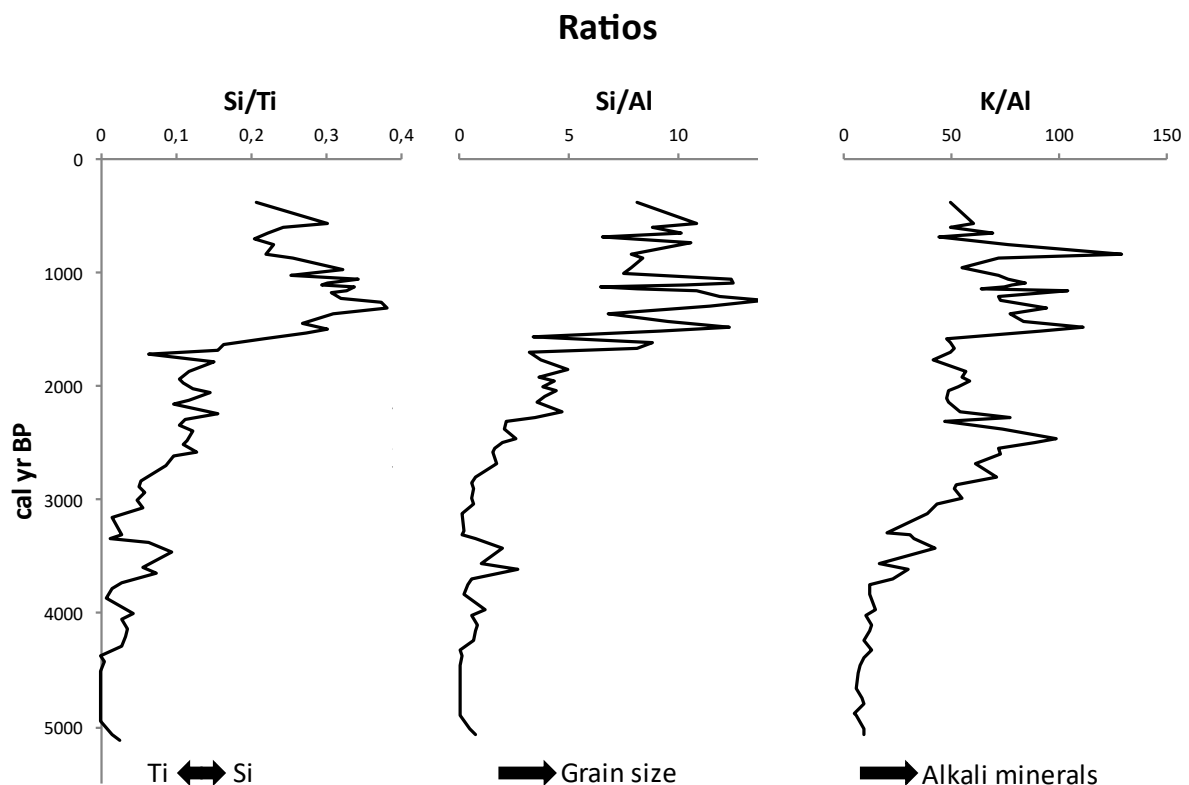


Figure 6. Elemental ratios based on pa values from XRF-CS.

3.6 Biplots of elemental data

Biplots for elements with positive association with PC2₅₁₀₀ (Si, Ti, Al and K) were made (Fig 7). Four periods (2300-1680, 1540-1440, 1300-1170 and 700-900 cal yr BP) with strong communality within periods was observed. The period 2300-1680 cal yr BP is more isolated from the other periods where some overlap is seen.

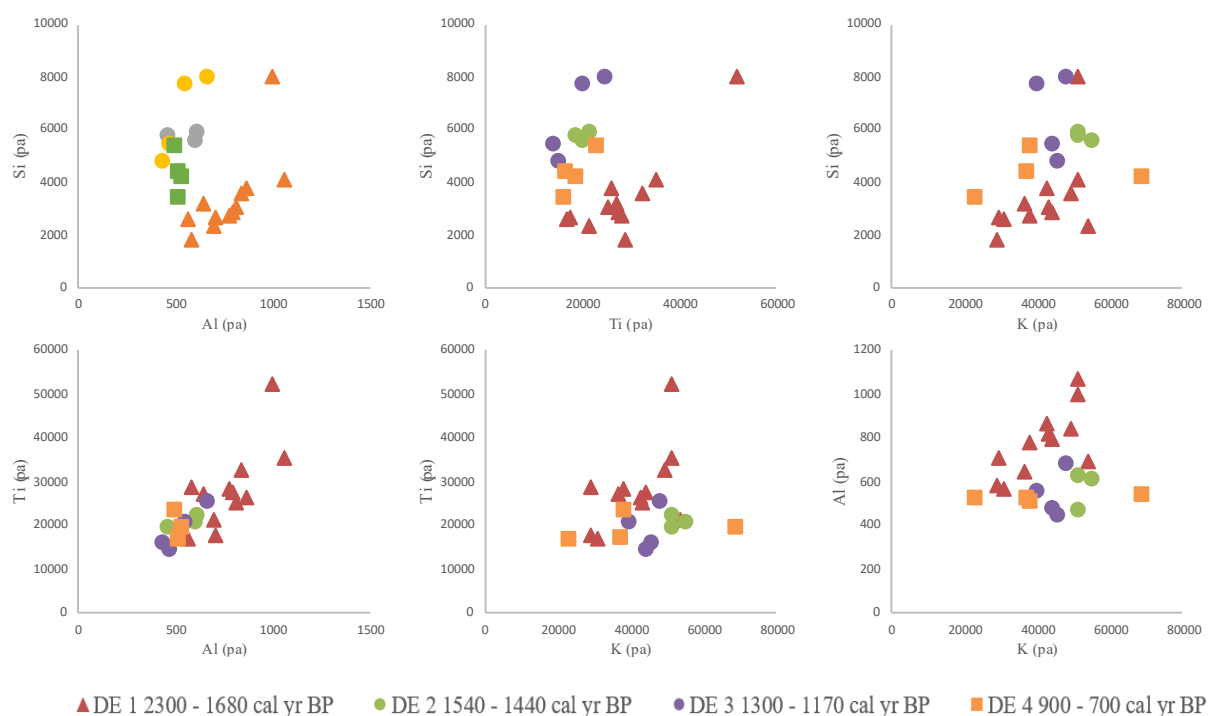


Figure 7. Elemental biplots of Si, Al, K and Ti during periods of positive factor scores from PC2₅₁₀₀ (Fig 5).

4. Discussion

4.1 Peatland Development

The bulk density range (0.04-0.30 g/cm³), average peat growth (0.95 mm/yr) and PAR (43.2-243.4 g/m²/yr) found in SM-DN sequence are generally higher compared with those found in previous studies at Store Mosse (0.017-0.15 g/cm³, 0.79 mm/yr and 13-189 g/m²/yr, Kylander et al., 2013; (0.033-0.137 g/cm³, 0.89 mm/yr and 25-125 g/m²/yr; Gåling, 2019). Higher average peat growth are seen for SM-DN and SM-DS whereas lower average peat growth is seen in SM-S (Kylander et al., 2013). This is also reflected in the PAR which is governed by several factors, including temperature, humidity/moisture, hydrology and nutrient availability (Loisel et al., 2014). It can be expected that the temperature and moisture content will be approximately equal over Store Mosse. The difference in PAR between the sites might be linked to differences in hydrology, but further studies are needed.

Peat accumulation at Store Mosse started ca 8500 cal yr BP in the southernmost part of Store Mosse (Kylander et al., 2013) compared to the SM-DN core where peat accumulation started

5200 cal yr BP. The later peat accumulation start at the SM-DN site is believed to be a result of sand dune movement with peat accumulation surrounding the dunes only proceeding after dune emplacement (Gåling, 2019). Optically stimulated luminescence (OSL) dating performed in a study by Bjerme (2019) found that dune emplacement at Store Mosse likely occurred 8-6 ka, which explains the younger age of the peat in the northern area of Store Mosse.

The age-depth model presented for SM-DN is built on only two ^{14}C dates, generating a near linear age model. This explains the strong co-variability between PAR and bulk density. Additional ^{14}C dates are needed to create a more robust age-depth model. However, the age-depth model for the SM-DS core, which is built on 5 ^{14}C dates, is similarly near-linear. This means that the SM-DN age might not be unrealistic despite its low resolution.

The oldest part of the SM-DN sequence contained wood fragments. This indicates that peatland initiation occurred through paludification, which is a common initiation process for mires in western Sweden (Svensson, 1988). The fen-bog transition started at 3900 cal yr BP and was complete by 3400 cal yr BP. This is evidenced by a simultaneous decrease in the bulk density, mobile (redox sensitive) elements and ash content at 3900 cal yr BP. This, in combination with the result from PC1₅₁₀₀ (explained below), which shows a transition from positive to negative scores at 3400 cal yr BP, indicates the system became ombrotrophic. A rapid decrease in bulk density implies a shift in vegetation, from *Carex* peat in the fen (high bulk density) to *Sphagnum* peat (low density) (Svensson, 1988). This change in vegetation suggests that the environmental conditions in the bog have changed, from a minerotrophic fen (nutrient rich) to an ombrotrophic bog (nutrient poor).

The input of flowing water contributes nutrients and minerals, which are reflected in the higher ash content at the base of the SM-DN core until 3400 cal yr BP after which the ash content is < 1% throughout the rest of the profile. The ombrotrophic stage of peatlands generally has low ash content (Tolonen, 1984), thus the low amount ash content from 3400 cal yr BP to present is interpreted to be from atmospheric deposition only. The minerotrophic status leading up to 3400 cal yr BP sees the input of minerals from fluvial sources which likely overprints or mix with the atmospheric signals (Kylander et al., 2013). Thus, the record before 3400 cal yr BP not suitable for dust reconstruction.

4.2 Interpretations of the geochemical signals in the SM-DN peat core

Elemental concentrations in peat paleoarchives can give good indications as to the different kinds of environmental processes that prevailed during a given time. PCA was used to explain the variability within the dataset. This allowed identification of variables with similar behaviour which can therefore be interpreted to be controlled by the same process. Two different PCA were run using the entire sequence, PC₅₁₀₀, as well as the ombrotrophic section, PC₃₄₀₀. Both PCs associate elements considered mobile (Mn, Fe, Rb) in PC1₅₁₀₀ and PC1₃₄₀₀, respectively. PC₃₅₁₀₀ and PC₂₃₄₀₀ both associated elements linked to pollution and anthropogenic activities (Cu, Zn, Pb). Conservative lithophile elements (Al, Si, K, Ti) are used as proxies for atmospheric mineral dust input (Kylander et al., 2020; Sjöström et al., 2020). In this study, these elements are associated with one factor (PC₂₅₁₀₀), covering the whole sequence and two factors (PC₃₃₄₀₀ and PC₄₃₄₀₀), when considering the ombrotrophic part of the sequence only.

Both PCs grouped Mn, Fe, Rb, and ash content (bulk density was included in PC1₅₁₀₀ only)

(Tables 1 and 2). PC1₅₁₀₀ shows high scores in the oldest part of the sequence which transition to negative scores at 3400 cal yr BP (Fig 5). The associated elements are considered mobile within the peat profile because of their redox-sensitive or soluble nature. These elements strongly vary with fluctuations in the water table. Iron for example is more abundant in the fen because the Fe supply comes from the basal sediments and soils through fluvial processes. With the higher water table anaerobic conditions prevail, thus the Fe won't oxidise (Shotyk, 1988). The elements found in both PCs are also associated with phases that are soluble in acidic reducing environments (Sjöström et al., 2020) and therefore get easily washed out. The bulk density and ash content in PC1₅₁₀₀ reflect the higher density in the fen (due to the increased decomposition in the presence of more oxygen) and the increased mineral input from fluvial sources to the fen, respectively. In the bog these elements persist from 3400 cal yr BP until they shift to negative values at 2600 cal yr BP.

PC2₅₁₀₀ is strongly associated with Al, Si, K, Ti and Sr which are all lithogenic elements that have a conservative biochemical nature. The association between Al, K, Si and Ti, suggest that they are hosted in the same mineral matrices, which makes these elements useful for identifying grain size variation and potential changes in dust sources. Silica can be of lithogenic or biogenic origin, for example from diatoms which are common in aquatic settings. However, a significant biogenic origin is not likely due to the strong association with Ti, Al and K (Table 1). Potassium is a common constituent in feldspars and micas (muscovite and biotite). These minerals are however subject to chemical weathering (dissolution) because of the low pH within the bog (Wilson, 2004). Since PC2₅₁₀₀ shows associations of K with the other lithophile elements it can be concluded that K is retained in the peat, even when to some extent K is an essential nutrient for plants (Wang et al., 2016) and therefore is subject to recycling within the peat.

Three ratios, Si/Ti, Si/Al and K/Al were plotted for the peat sequence (Fig. 6). From a nearby combined soil and peat study (Davidsmossen, ca 60 km away), Sjöström (2020) found that the Si/Ti ratio could be used to reflect changes in mineral composition for quartz and feldspars (Si) and heavy minerals like ilmenite (Ti). The same study found that a higher Si/Al ratio coincided with the presence of quartz and feldspar. Quartz and feldspar minerals are both associated with coarser grain sizes (Glaccum and Prospero, 1980) and therefore the Si/Al ratio is associated with changes in grain size where an increase represents coarser grain sizes. The K/Al ratio show a similar trend as Si/Ti and Si/Al except for the period between 2300-1600 cal yr BP where the ratio drops. Potassium and Al are common constituents in feldspar and micas, thus suggesting that the K/Al ratio represents alkali mineral input.

In PC₃₄₀₀ the conservative lithophile elements are split up into two factors: PC₃₄₀₀ and PC₄₃₄₀₀. PC₃₄₀₀ associates Al, Ti, Sr and ash content (Table 2) and positive scores are only seen 2300-1680 cal yr BP. In PC₃₄₀₀ K is not associated with Al, thus indicating that some process or processes are reducing the available K in the sequence or a different source is supplying the bog. It is suggested here that the Al sits in fine grained clay minerals because the absence of K. The strong association of Al and Ti from 2300-1600 cal yr BP coincide with low values in the Si/Ti, Si/Al and K/Al ratio and is therefore PC₃₄₀₀ interpreted to represent input of clays and heavy minerals.

The PC₄₃₄₀₀ profile, associated with Si, K and Ti, exhibits ten shorter periods of elevated values which coincide with peaks in Si/Al (Fig 8). This suggest that larger grains size fraction were deposited during these periods. The K/Al ratio shows a similar trend to the Si/Al ratio except for the period between 2300-1600 cal yr BP. A higher K/Al ratio suggests that more K-

feldspars and micas are present within the sequence. Since Si is strongly associated with K, but only to some extent with Al (table 2), it is suggested here that the observed peaks in PC₄₃₄₀₀ mainly represent input of coarse-grained quartz and to some extent alkali minerals (feldspars).

PC₃₅₁₀₀ and PC₂₃₄₀₀ are associated with the metals Cu, Zn and Pb (Tables 2 and 3). The strong increase at the top of the profile with high positive scores for these elements combined with the negative scores from the base to 2300 cal yr BP suggests that the source of these elements is anthropogenic. These elements are associated as pollution metals which are being put into the atmosphere mainly by mining. The small peak at 2300 cal yr BP might be related to increased mining during the Roman empire (Kylander et al., 2020).

4.3 Dust Events

In the fen section of the sequence dust signals might be blurred by incoming material from fluvial sources as reflected in the ash profile. Active fluvial transport during the fen stage may be expected to increase Si/Al ratios with larger grains being able to be transported. However, the local topography, basin of deposition, sample location along with other factors might mean that larger grained detrital material was not carried via fluvial transport to the sampling site. In order to understand as well as exclude any potential fluvial input of detrital minerals, two PCA were conducted: one over the whole sequence (PC₅₁₀₀) and the other only in the ombrotrophic section (PC₃₄₀₀). Since the bog stage is exclusively atmospherically fed, and this reflects atmospheric minerals dusts, the focus here is to identify periods of increased minerogenic deposition after 3400 cal yr BP.

In order to identify periods of increased atmospheric dust deposition this study used positive values from PC₂₅₁₀₀ since it captured all lithogenic elements. A total of four DE were identified in the SM-DN core: DE1:2300-1680, DE2:1540-1440, DE3:1300-1170 and DE4:900-700 cal yr BP (Fig 8). PC₃₃₄₀₀ and PC₄₃₄₀₀ was used to identify changes within the lithogenic elements themselves, and specifically, their mineralogy, where PC₃₃₄₀₀ indicates clay and heavy minerals while PC₄₃₄₀₀ show quartz and feldspar. The ash content is generally low throughout the ombrotrophic part of the profile even when increases in grain size (Si/Al) is observed. Biplots of the lithogenic elements Si, Ti, Al and K indicates that the composition of the mineral dust was different during the DE (Fig 7). Most noticeable is that DE1 has almost no overlap with DE2, DE3 and DE4, thus indicating that DE1 was supplied from a different source. Some overlap is seen the biplots of DE2, DE3 and DE4 which suggest a more similar mineral composition and thus, source.

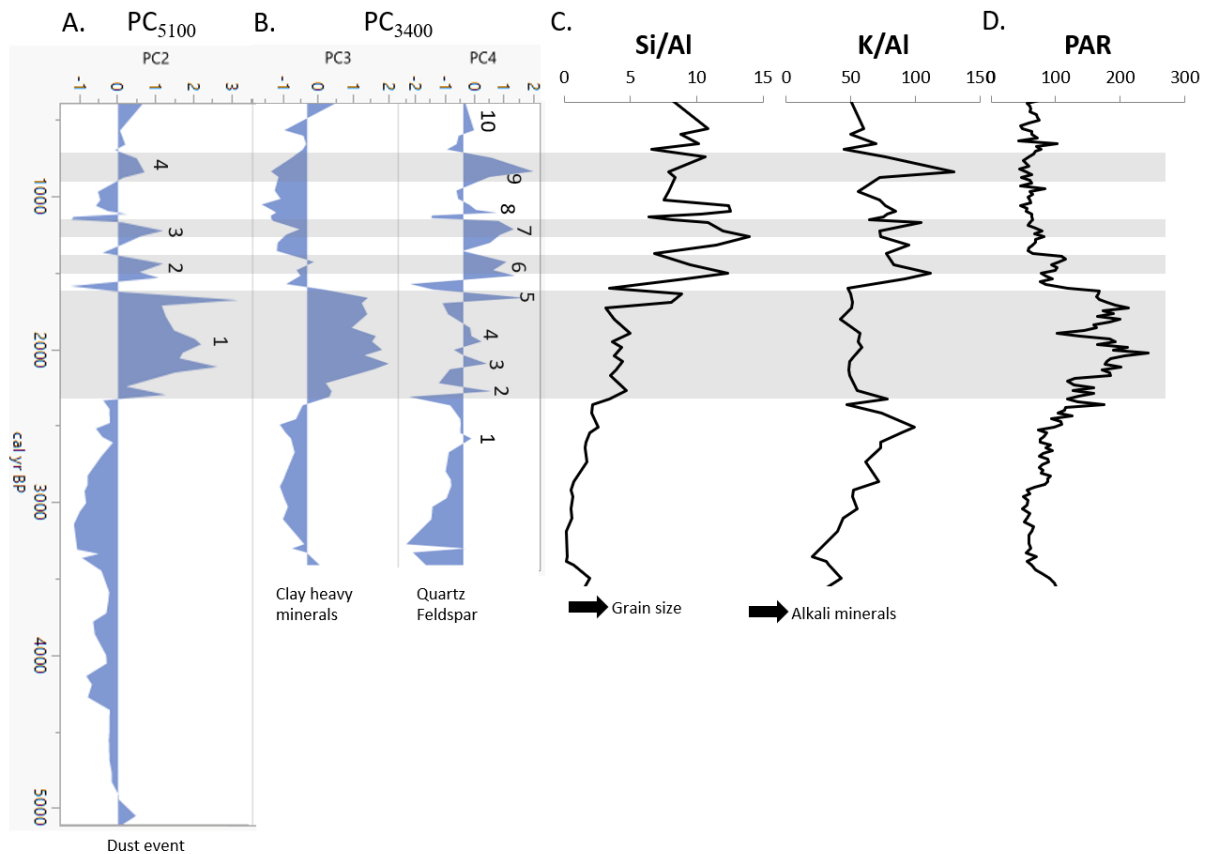


Figure 8. Summary figure of dust events. A) Dust events interpreted from PC2₅₁₀₀. B) Interpreted mineral composition from PC3₃₄₀₀ and PC4₃₄₀₀. All observed peaks in PC3₃₄₀₀ are numbered from 1-10. C) Grain size changes and changes in alkali mineral input. D) PAR. Grey areas indicates the four different dust events.

During DE1, PC3₃₄₀₀ found strong association between Al, Ti, Sr and ash content extending over the entire period, while PC4₃₄₀₀ showed only 4 small peaks associated with Si, K and Ti. Biplots (Fig 7.) suggest that the dust deposition during this time was mainly from one source. But, because some overlap is seen in the biplots and between PC3₃₄₀₀ and PC4₃₄₀₀, other sources cannot be excluded. The low values seen in the Si/Ti ratio indicates that heavy minerals are present during DE1. A small increase above background noise is seen in the Si/Al ratio, suggesting that larger grain sizes were deposited. The K/Al ratio show a rapid drop during DE1 which suggest that the alkali mineral input was low. In relation to low alkali mineral input, PAR values show an opposite behaviour; they are strongly elevated (Fig 8). In PC3₃₄₀₀, the strong association between Ti and Al, together with a small increase in grain size, and only low amounts of alkali minerals, suggest that DE1 is associated with finer grain sizes of clay and heavy minerals (ilmenite).

During DE1, cooler and drier climate prevailed over Store Mosse (Kylander et al., 2013), thus making soils and clays more available for aeolian transport. Kylander et al. (2016) recognized increased input of clays and heavy minerals between 2380-2200 cal yr BP which are thought to be a mix of local and regional derived dust. Pollen records from studies by Lagerås (1996) and Jong et al. (2006) found that agriculture was an ongoing process in Store Mosse during DE1, which might explain a local source. The source of regional dust though, is unknown. Rather than PAR increase depending on warmer and wetter climate as well as a fluctuating water table (Bengtsson et al., 2020), it is here suggested that increased aeolian transport of dust enriched in nutrients might be responsible for the increase seen under DE1.

The increase in peat growth might explain the drop in K/Al ratio. Since K is an essential nutrient for plants (Wang et al., 2016), this might reduce the available K in the bog.

DE2-DE4 share a similar pattern. The peaks of elemental ratios coincide with elevated values in PC₄₃₄₀₀. This indicates that coarser grain size of quartz and alkali minerals were deposited, and only small portions of heavy minerals were present. Grain size can be used as an indicator of storminess since stronger winds have potential to carry larger particles (Jong et al., 2006). Closer spacing in the biplots are seen for DE2-DE4, indicating a more similar mineral composition.

Pollen from *Cerealia* can be used to track anthropogenic agriculture. In a study by T. Mighall (SM-S unpublished data) the first occurrence of *Cerealia* pollen at Store Mosse was dated to ca 1600 cal yr BP with increasing values towards present. Agricultural processes make soil and sediment more susceptible to aeolian transport as well as opens the landscape, making it more exposed to winds. This can be an explanation of source origin for the minerals deposited during DE2, DE3 and DE4. The huge variability in Si/Al and K/Al ratios during these DE thus indicates that the energy of the storms shifted dramatically during these periods. PC₄₃₄₀₀ show positive scores for DE2, DE3 and DE4 which suggests that the main coarse mineral deposited during these periods were quartz and to some extent K-feldspars since Al is only moderately associated with Si, K and Ti in PC₄₃₄₀₀. DE2-DE4 are therefore associated with larger grain sizes of quartz and alkali minerals (feldspars).

4.4 Comparison with other paleoenvironmental records

Besides creating a paleodust record, this project also aims to understand the peatland development in the northernmost part of Store Mosse. To date, only one core, SM-DS, has been analysed in a study by Gåling (2019). Some apparent differences in analytical approach between SM-DN and SM-DS core are found. Firstly, the sample resolution used for organic (1 cm), and inorganic (2-3 cm) analyses were higher in the SM-DS core compared to SM-DN (2 cm and 5 cm, respectively). Secondly, the XRF-CS dataset for each site did not contain the same elements, thus elements may or may not affect association between PCA and thus associates variables differently.

Elevated values in PC₄₃₄₀₀ from the SM-DN core identified mainly quartz grains. In a study, Björck and Clemmensen (2004) used the Aeolian Sand Influx (ASI) to measure variation in grains larger than 200 μm over time. They systematically counted quartz grains from two peatbogs (Boarps Mosse and Hyltemossen) located in Halland, Sweden to determine the variation in the ASI and found elevated ASI values over the last 2500 cal yr BP. The timing of peak values in PC₄₃₄₀₀, ASI peaks from Björck and Clemmensen (2004) and periods of increased grain size in the SM-DS core (Gåling, 2019) are compared in Table 3. The SM-DN record does not have data for the periods before 400 cal yr BP. However, 7 out of 9 of the observed peaks coincide between SM-DN and SM-DS, and 9 of the periods for SM-DN coincide with higher influx of coarse-grained quartz in Boarpsmosse and Hyltemosse. A possible explanation for the differences seen between SM-DN and SM-DS might be the proximity to the dunes. However, to further interpret the source of the mineral grains, grain size and microscope analysis could be used to determine roundness.

The timing of the identified DEs in this study follow to some extent a general storminess patterns seen on a larger scale. In Sorrel et al. (2012) records from coastal regions across northern Europe were studied and compiled in order to identify stormier periods. They

identified five widespread stormy intervals: 5800-5500, 4500-3950, 3300-2400, 1900-1050 and 600-250 cal BP using OSL dating on dunes. The record for SM-DN, beginning in 5200 cal yr BP, show no signs of increased grain size until 2650 cal yr BP. Some overlap is seen in the period 1900-1050, where three out of four DE were identified in the SM-DN core. However, it's important to point out that increased dust deposition is not always connected to storms. Given the fact that windier conditions prevail in coastal sites than in inland sites, Sorrel's study might not be the optimal comparing material. Although, by comparing with Sorrel, there is a possibility to reflect upon the more general global variations in storminess.

Table 3.

Peak values from PC4₃₄₀₀ from SM-DN compared to peaks from SM-DS and peaks in ASI from (Björck and Clemmensen, 2004).

SM-DN peaks (cal yr BP)	SM-DS peaks (cal yr bp)	ASI peaks (cal yr BP)
No record	250-150, 400-385	130, 300 , 400
590-420	-	475
950-720	710-625	900
1120-1040	-	1100, 1150
1370-1160	1330-1265	1350
1560-1370	1690-1455	1450
1700-1640	1690-1455	1675
2020-1850	1905-1780	1875
2150-2060	2310-2025	2150
2380-2270	2310-2025	2300
2650-2590	-	-

5. Conclusions

The aim of this project was to reconstruct paleoenvironmental conditions in the northern part of Store Mosse over the last 5200 cal yr BP by identifying changes in peat properties and atmospheric dust deposition. Analysis of bulk density, PAR and ash content suggests that the peatland started the transition from a fen to bog at 3900 cal yr BP and was fully ombrotrophic at 3400 cal yr BP. This was further supported by shifts in mobile elements (PC1₅₁₀₀).

Atmospheric signals at SM-DN are likely overprinted before 3400 cal yr BP because of the minerotrophic status of the fen. Multiple proxies were used to determine past dust deposition. Bulk density, ash content and a suite of 11 elements were statistically evaluated using PCA to identify periods of increased dust deposition. Four periods of increased dust deposition, denoted DE1-DE4 (2300-1680, 1540-1440, 1300-1170 and 900-700 cal yr BP respectively) was identified based on change in PC2₅₁₀₀. DE1 is associated with finer grain sizes of clay and heavy minerals (ilmenite) while DE2-DE4 are associated with larger grain sizes, quartz and alkali minerals (feldspars).

A total of ten periods of increased quartz and feldspar deposition, which represents the coarsest grain size in this study was interpreted from PC4₃₄₀₀. These periods are short lived and

interpreted as periods of increased storminess. Good agreement in these periods are seen in a nearby record, SM-DS and from ombrotrophic bogs ca 90 km southwest of Store Mosse, thus suggesting that the storms were of regional scale.

Acknowledgement

First and foremost, I would like to thank my supervisor Malin Kylander for her excellent support and motivation during this project. Carina Johansson is thanked for guiding me around in the lab and for great help during freeze-drying and ashing of samples. Lastly, I want to thank my sister Ebba Vikdahl for proof-reading my English.

5. References

- Albani, S., Mahowald, N.M., Winckler, G., Anderson, R.F., Bradtmiller, L.I., Delmonte, B., François, R., Goman, M., Heavens, N.G., Hesse, P.P., Hovan, S.A., Kang, S.G., Kohfeld, K.E., Lu, H., Maggi, V., Mason, J.A., Mayewski, P.A., McGee, D., Miao, X., Otto-Bliesner, B.L., Perry, A.T., Pourmand, A., Roberts, H.M., Rosenbloom, N., Stevens, T., Sun, J., 2015. Twelve thousand years of dust: the Holocene global dust cycle constrained by natural archives. *Clim. Past* 11, 869–903. <https://doi.org/10.5194/cp-11-869-2015>
- Bengtsson, F., Granath, G., Cronberg, N., Rydin, H., 2020. Mechanisms behind species-specific water economy responses to water level drawdown in peat mosses. *Ann. Bot.* 126, 219–230. <https://doi.org/10.1093/aob/mcaa033>
- Björck, S., Clemmensen, L., 2004. Aeolian sediment in raised bog deposits, Halland, SW Sweden: A new proxy record of Holocene winter storminess variation in southern Scandinavia? *Holocene* 14, 677–688. <https://doi.org/10.1191/0959683604hl746rp>
- Blytt, A., 1876. Essay on the Immigration of the Norwegian Flora During Alternating Rainy and Dry Periods. A. Cammermeyer.
- Franzén, L.G., 2006. Chapter 11 Mineral matter, major elements, and trace elements in raised bog peat: a case study from southern Sweden, Ireland and Tierra del Fuego, south Argentina, in: Martini, I.P., Martínez Cortizas, A., Chesworth, W. (Eds.), *Developments in Earth Surface Processes, Peatlands*. Elsevier, pp. 241–269. [https://doi.org/10.1016/S0928-2025\(06\)09011-0](https://doi.org/10.1016/S0928-2025(06)09011-0)
- Glaccum, R., Prospero, J., 1980. Saharan Aerosols Over the Tropical North-Atlantic - Mineralogy. *Mar. Geol.* 37, 295–321. [https://doi.org/10.1016/0025-3227\(80\)90107-3](https://doi.org/10.1016/0025-3227(80)90107-3)
- Ising, J., 2001. Late Weichselian pollen stratigraphy, clay varve chronology and palaeomagnetic secular variations in Lake Bolmen, Småland, south Sweden. *Boreas* 30, 189–204. <https://doi.org/10.1111/j.1502-3885.2001.tb01222.x>
- Jong, R. de, Björck, S., Björkman, L., Clemmensen, L.B., 2006. Storminess variation during the last 6500 years as reconstructed from an ombrotrophic peat bog in Halland, southwest Sweden. *J. Quat. Sci.* 21, 905–919. <https://doi.org/10.1002/jqs.1011>
- Kohfeld, K.E., Harrison, S.P., 2001. DIRTMAP: the geological record of dust. *Earth-Sci. Rev.*, Recent research on loess and palaeosols, pure and applied 54, 81–114. [https://doi.org/10.1016/S0012-8252\(01\)00042-3](https://doi.org/10.1016/S0012-8252(01)00042-3)
- Kylander, M.E., Bindler, R., Cortizas, A.M., Gallagher, K., Mörth, C.-M., Rauch, S., 2013. A novel geochemical approach to paleorecords of dust deposition and effective humidity: 8500 years of peat accumulation at Store Mosse (the “Great Bog”), Sweden. *Quat. Sci. Rev.* 69, 69–82. <https://doi.org/10.1016/j.quascirev.2013.02.010>

- Kylander, M.E., Martínez-Cortizas, A., Bindler, R., Greenwood, S.L., Mörth, C.-M., Rauch, S., 2016. Potentials and problems of building detailed dust records using peat archives: An example from Store Mosse (the “Great Bog”), Sweden. *Geochim. Cosmochim. Acta* 190, 156–174. <https://doi.org/10.1016/j.gca.2016.06.028>
- Kylander, M.E., Martínez-Cortizas, A., Bindler, R., Kaal, J., Sjöström, J.K., Hansson, S.V., Silva-Sánchez, N., Greenwood, S.L., Gallagher, K., Rydberg, J., Mörth, C.-M., Rauch, S., 2018. Mineral dust as a driver of carbon accumulation in northern latitudes. *Sci. Rep.* 8, 6876. <https://doi.org/10.1038/s41598-018-25162-9>
- Kylander, M.E., Söderlindh, J., Schenk, F., Gyllencreutz, R., Rydberg, J., Bindler, R., Cortizas, A.M., Skelton, A., 2020. It’s in your glass: a history of sea level and storminess from the Laphroaig bog, Islay (southwestern Scotland). *Boreas* 49, 152–167. <https://doi.org/10.1111/bor.12409>
- Lagerås, P., 1996. Farming and forest dynamics in an agriculturally marginal area of southern Sweden, 5000 BC to present: a palynological study of Lake Avegöl in the Småland Uplands. *The Holocene* 6, 301–314. <https://doi.org/10.1177/095968369600600305>
- Lambert, F., Delmonte, B., Petit, J.R., Bigler, M., Kaufmann, P.R., Hutterli, M.A., Stocker, T.F., Ruth, U., Steffensen, J.P., Maggi, V., 2008. Dust-climate couplings over the past 800,000 years from the EPICA Dome C ice core. *Nature* 452, 616–619. <https://doi.org/10.1038/nature06763>
- Loisel, J., Yu, Z., Beilman, D.W., Camill, P., Alm, J., Amesbury, M.J., Anderson, D., Andersson, S., Bochicchio, C., Barber, K., Belyea, L.R., Bunbury, J., Chambers, F.M., Charman, D.J., De Vleeschouwer, F., Fiałkiewicz-Kozielec, B., Finkelstein, S.A., Gałka, M., Garneau, M., Hammarlund, D., Hinchcliffe, W., Holmquist, J., Hughes, P., Jones, M.C., Klein, E.S., Kokfelt, U., Korhola, A., Kuhry, P., Lamarre, A., Lamentowicz, M., Large, D., Lavoie, M., MacDonald, G., Magnan, G., Mäkilä, M., Mallon, G., Mathijssen, P., Mauquoy, D., McCarroll, J., Moore, T.R., Nichols, J., O’Reilly, B., Oksanen, P., Packalen, M., Peteet, D., Richard, P.J., Robinson, S., Ronkainen, T., Rundgren, M., Sannel, A.B.K., Tarnocai, C., Thom, T., Tuittila, E.-S., Turetsky, M., Väliranta, M., van der Linden, M., van Geel, B., van Bellen, S., Vitt, D., Zhao, Y., Zhou, W., 2014. A database and synthesis of northern peatland soil properties and Holocene carbon and nitrogen accumulation. *The Holocene* 24, 1028–1042. <https://doi.org/10.1177/0959683614538073>
- Longman, J., Veres, D., Wennrich, V., 2019. Utilisation of XRF core scanning on peat and other highly organic sediments. *Quat. Int., Advances in Data Quantification and Application of high resolution XRF Core Scanners* 514, 85–96. <https://doi.org/10.1016/j.quaint.2018.10.015>
- Lundqvist, J., Wohlfarth, B., 2000. Timing and east–west correlation of south Swedish ice marginal lines during the Late Weichselian. *Quat. Sci. Rev.* 20, 1127–1148. [https://doi.org/10.1016/S0277-3791\(00\)00142-6](https://doi.org/10.1016/S0277-3791(00)00142-6)
- Pye, K., 1987. Chapter Six - GRAIN SIZE, MINERALOGY AND CHEMICAL COMPOSITION OF AEOLIAN DUST. Elsevier.
- Shao, Y., Wyrwoll, K.-H., Chappell, A., Huang, J., Lin, Z., McTainsh, G.H., Mikami, M., Tanaka, T.Y., Wang, X., Yoon, S., 2011. Dust cycle: An emerging core theme in Earth system science. *Aeolian Res.* 2, 181–204. <https://doi.org/10.1016/j.aeolia.2011.02.001>
- Shaw, T.A., Baldwin, M., Barnes, E.A., Caballero, R., Garfinkel, C.I., Hwang, Y.-T., Li, C., O’Gorman, P.A., Rivière, G., Simpson, I.R., Voigt, A., 2016. Storm track processes and the opposing influences of climate change. *Nat. Geosci.* 9, 656–664. <https://doi.org/10.1038/ngeo2783>

- Shotyk, W., 1988. Review of the inorganic geochemistry of peats and peatland waters. *Earth-Sci. Rev.* 25, 95–176. [https://doi.org/10.1016/0012-8252\(88\)90067-0](https://doi.org/10.1016/0012-8252(88)90067-0)
- Sjöström, J.K., Martínez Cortizas, A., Hansson, S.V., Silva Sánchez, N., Bindler, R., Rydberg, J., Mörth, C.-M., Ryberg, E.E., Kylander, M.E., 2020. Paleodust deposition and peat accumulation rates – Bog size matters. *Chem. Geol.* 554, 119795. <https://doi.org/10.1016/j.chemgeo.2020.119795>
- SMHI (Swedish metrological and hydrological institute)., 2021. Internet. <https://www.smhi.se/data/meteorologi/ladda-ner-meteorologiska-observationer/#param=airTemperatureMeanMonth,stations=all,stationid=74180> (accessed 19 April 2021)
- Sorrel, P., Debret, M., Billeaud, I., Jaccard, S.L., McManus, J.F., Tessier, B., 2012. Persistent non-solar forcing of Holocene storm dynamics in coastal sedimentary archives. *Nat. Geosci.* 5, 892–896. <https://doi.org/10.1038/ngeo1619>
- Svensson, G., 1988. Bog development and environmental conditions as shown by the stratigraphy of Store Mosse mire in southern Sweden. *Boreas* 17, 89–111. <https://doi.org/10.1111/j.1502-3885.1988.tb00126.x>
- Geological Survey of Sweden., 2020a. Internet. <https://www.sgu.se/produkter/kartor/kartvisaren/bergkartvisare/berggrund-11-miljon/> (accessed: 10 May 2021)
- Geological Survey of Sweden., 2020b. Internet. <https://www.sgu.se/produkter/kartor/kartvisaren/jordkartvisare/jordarter-125-000-1100-000/> (accessed: 10 May 2021)
- Tolonen, K., 1984. Interpretation of changes in the ash content of ombrotrophic peat layers. *Bull. Geol. Soc. Finl.* 56, 207–219. <https://doi.org/10.17741/bgsf/56.1-2.013>
- Vandel, E., Vaasma, T., Sugita, S., Tõnisson, H., Jaagus, J., Vilumaa, K., Anderson, A., Kont, A., 2019. Reconstruction of past storminess: Evaluation of an indicator approach using aeolian mineral grains buried in peat deposits, Estonia. *Quat. Sci. Rev.* 218, 215–227. <https://doi.org/10.1016/j.quascirev.2019.06.026>
- Wang, M., Larmola, T., Murphy, M.T., Moore, T.R., Bubier, J.L., 2016. Stoichiometric response of shrubs and mosses to long-term nutrient (N, P and K) addition in an ombrotrophic peatland. *Plant Soil* 400, 403–416. <https://doi.org/10.1007/s11104-015-2744-6>
- Wilson, M.J., 2004. Weathering of the primary rock-forming minerals: processes, products and rates. *Clay Miner.* 39, 233–266. <https://doi.org/10.1180/0009855043930133>

6. Appendix

Appendix A, Fresh core photos



Figure A1. Fresh photos of SMDN core. From the top to the base, C1) 50-150 cm, C2) 125-225 cm, C3) 200-300 cm, C4) 275-375 cm, C5) 350-450 cm, C6) 408-508 cm. Photos taken by Malin Kylander.

Appendix B, Elemental profiles

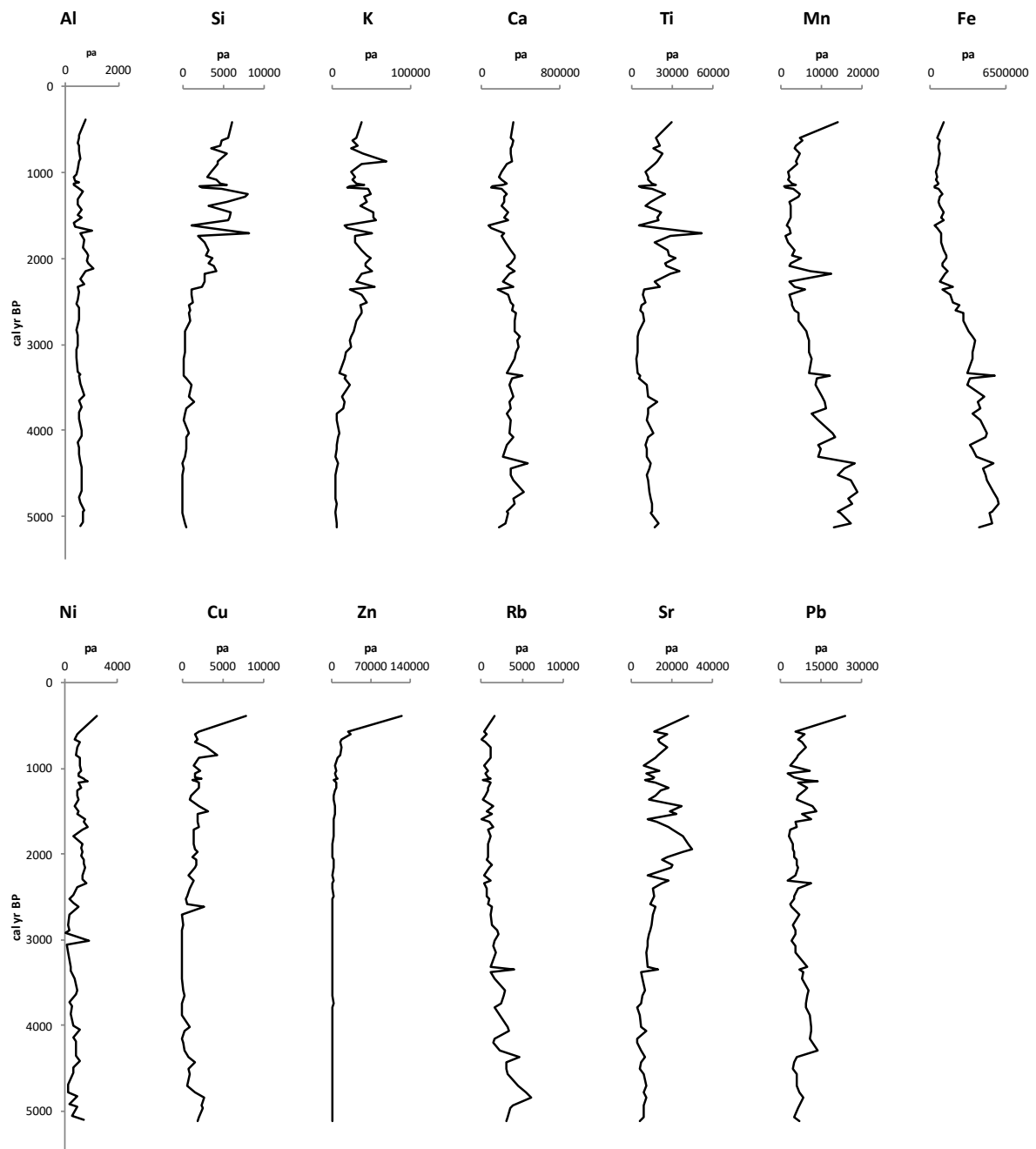


Figure B1. Elemental profiles from XRF-CS on ashed peat.